Lysozyme activity of the *Ruminococcus champanellensis* cellulosome

Sarah Moraïs[1], Darrell W. Cockburn[2], Yonit Ben-David[1], Nicole M. Koropatkin[2], Eric C. Martens[2], Sylvia H. Duncan[3], Harry J. Flint[3], Itzhak Mizrahi[4] and Edward A. Bayer[1*]

[1]*Biomolecular Sciences Department, The Weizmann Institute of Science, Rehovot, Israel.*

[2]*Department of Microbiology and Immunology, University of Michigan Medical School, Ann Arbor, Michigan 48109, USA.*

[3]*Microbiology Group, Rowett Institute of Nutrition and Health, University of Aberdeen, Aberdeen, United Kingdom.*

[4] *The Department of Life Sciences & the National Institute for Biotechnology in the Negev, Ben-Gurion University of the Negev, Beer-Sheva 84105, Israel.*

*Corresponding author:
Edward A. Bayer, Department of Biological Chemistry, The Weizmann Institute of Science, Rehovot, Israel. Tel: (+972)-8-934-2373. Fax: (+972)-8-934-4118.
Email: ed.bayer@weizmann.ac.il

Running head: *Ruminococcus champanellensis* cellulosomal lysozyme

This is the author manuscript accepted for publication and has undergone full peer review but has not been through the copyediting, typesetting, pagination and proofreading process, which may lead to differences between this version and the Version record. Please cite this article as doi:10.1111/1462-2920.13501.

Originality-Significance Statement

This work deals with the identification of a cellulosomal cohesin-containing scaffoldin, which includes a family 25 glycoside hydrolase enzyme that exhibits lysozyme activity. This is the first example of a bacterial lysozyme produced as part of the cellulosome apparatus.

Abstract

Ruminococcus champanellensis is a keystone species in the human gut that produces an intricate cellulosome system of various architectures. A variety of cellulosomal enzymes have been identified, which exhibit a range of hydrolytic activities on lignocellulosic substrates. We describe herein a unique *R. champanellensis* scaffoldin, ScaK, which is expressed during growth on cellobiose and comprises a cohesin module and a family 25 glycoside hydrolase (GH25). The GH25 is non-autolytic and exhibits lysozyme-mediated lytic activity against several bacterial species. Despite the narrow acidic pH curve, the enzyme is active along a temperature range from 2 to 85°C and is stable at very high temperatures for extended incubation periods. The ScaK cohesin was shown to bind selectively to the dockerin of a monovalent scaffoldin (ScaG), thus enabling formation of a cell-free cellulosome, whereby ScaG interacts with a divalent scaffodin (ScaA) that bears the enzymes either directly or through additional monovalent scaffoldins (ScaC and ScaD). The ScaK cohesin also interacts with the dockerin of a protein comprising multiple Fn3 domains that can potentially promote adhesion to carbohydrates and the bacterial cell surface. A cell-free cellulosomal GH25 lysozyme may provide a bacterial strategy to both hydrolyze lignocellulose and repel eventual food competitors and/or cheaters.

Introduction

Ruminococcus champanellensis is the sole known human gut bacterium able to degrade crystalline cellulose (Chassard et al., 2012). It produces a cellulosome that has been characterized recently (Ben David et al., 2015; Morais et al., 2015). Cellulosomes are large-molecular-weight enzymatic complexes that represent an extremely efficient strategy for cellulose and hemicellulose degradation (Bayer et al., 2004; Bayer et al., 2007; Himmel et al., 2010). The strong intermodular calcium-dependent cohesin/dockerin interaction drives the assembly between the cellulosomal enzymes and the central non-catalytic, integrating subunit, the scaffoldin, to form the mature complex (Yaron et al., 1995; Lytle et al., 1996). The *R. champanellensis* genome contains 12 scaffoldins with various molecular arrangements and specificities (Figure 1). The largest cellulosome that could be assembled by *R. champanellensis* would be composed of an anchoring scaffoldin, ScaE, comprising a sortase motif and a cohesin that can interact with the dockerin of a second scaffoldin, ScaB. The latter contains 7 cohesin modules, three of which interact either directly with dockerin-bearing enzymes, whereas the remainder can interact either with dockerin-bearing enzymes or with a third dockerin-bearing scaffoldin, ScaA. ScaA also contains two cohesin modules that interact either directly with dockerin-bearing enzymes or indirectly via monovalent scaffoldins (ScaC and ScaD) that play a role of molecular adaptors, thereby modulating the enzymatic composition of the cellulosome (Rincon et al., 2004; Ben David et al., 2015). The entire complex would thus contain a maximum of 11 enzymes. *R. champanellensis* contains a total of 65 dockerin-bearing proteins, 8 scaffoldin-borne dockerins (Ben David et al., 2015), 25 recently characterized glycoside hydrolases (Morais et al., 2015) and 31 additional dockerin-containing proteins. The *R. champanellensis* cellulosome thus presents a fined-tuned cohesin/dockerin recognition system that enables regulated assembly of an elaborate cellulosomal organization (Morais et al., 2015).

Unlike common scaffoldins that are non-enzymatic subunits, the ScaK scaffoldin carries an enzyme that is associated with the metabolism of cellular structural components, i.e., the peptidoglycan. ScaK is composed of a cohesin module (definitive of the scaffoldins) at its N-terminus and a GH25 catalytic domain in its C-terminal region. GH25 enzymes are retaining glycoside hydrolases that cleave the β-1,4-glycosidic bond between *N*-acetylmuramic acid (NAM) and N-acetylglucosamine

(NAG) in the carbohydrate backbone of bacterial peptidoglycan (i.e., lysozymes). Two main biological roles can be attributed to bacterial GH25 enzymes: the autolysis, the re-modeling of peptidoglycan in cellular growth processes, and the dissemination of phage progeny toward the end of the phage lytic cycle via lysis of the bacterial cell. These specialized hydrolases can also create enlarged pores in the bacterial peptidoglycan for the assembly of large trans-envelope complexes (e.g., pili, flagella, secretion systems) (Vollmer et al., 2008).

The genome of *Ruminococcus* sp. CAG:379 strain, closely related to *R. champanellensis,* also contains a gene encoding a protein homologous to ScaK with a similar modular arrangement (cohesin and GH25 modules). In additional *Ruminococcus* species, such as *R. bicirculans* and *R. flavefaciens* that carry multiple GH25 genes, the GH25 module is not accompanied by a cohesin module. ScaK also has 30% identity and 49% similarity with the GH25 module of LytC, an autolysin from *Streptococcus pneumoniae*, which is involved in a three-component mechanism for the lysis of sister cells non-competent for natural genetic transformation (Claverys et al., 2007; Monterroso et al., 2008; Eldholm et al., 2009). The fact that the ScaK GH25 module is connected to a cellulosomal element raises the question of possible lysozyme activity associated with the cellulosome that could provide a novel strategy that would prove beneficial for the bacterial cell.

In our previous report (Ben David et al., 2015), the ScaK cohesin was expressed as a CBM-fused cohesin (carbohydrate binding module) but was not found to bind any of the dockerin partners tested. In the present study, we cloned and expressed the ScaK scaffoldin as an intact wild-type protein, in an attempt to reveal potential cohesin affinity partners and to study the GH25 activity.

Results

Scaffoldin production and functionality of their cohesin modules

ScaK, ScaG and ScaF scaffoldins (Figure 1) were produced in *Escherichia coli,* purified on Ni-beads, and their estimated molecular weights were in good agreement with their calculated molecular masses (see legend to Supplemental Figure S1).

In order to understand the architectural context in which ScaK is positioned within the cellulosome, the dockerin specificities of the ScaK cohesin was examined by an affinity ELISA approach using the representative dockerin-bearing fusion proteins listed in Table 1. For this purpose, 12 dockerin modules were fused to a xylanase tag (xylanase T6 from *Geobacillus stearothermophilus*) that promotes solubility and expression of the dockerin and serves as a recognition tag for the primary antibody in the ELISA procedure (Barak et al., 2005)). The resultant xylanase-dockerin (Xyn-Doc) fusion proteins are listed in Table 1. All dockerins from the *R. champanellensis* scaffoldins (eight in total) were tested, since they represent the main backbones of its cellulosome structures. The four additional selected dockerins belonged to the 3 dockerin groups (Groups 1, 2 and 3-4) of cohesin-dockerin interactions in this bacterium, as previously defined using bioinformatic-based criteria (Ben David et al., 2015; Morais et al., 2015). ScaK, expressed as a full-length protein (lacking the signal peptide), was able to interact with the ScaG and protein 3939 dockerins (Figure 2A), in contrast to the previous report (Ben David et al., 2015), where the cohesin module was expressed alone, in the absence of the GH25 module.

ScaG is a scaffoldin that comprises only a cohesin and a dockerin (Figure 1). In a previous report (Ben David et al., 2015), the cohesin and dockerin modules of ScaG were expressed separately, the dockerin demonstrated binding activity for the first cohesin of ScaJ and ScaE, but the cohesin of ScaG failed to interact with any of the dockerin counterparts and was termed inactive in that study. We produced here the full ScaG protein length in an attempt to reveal the binding partner of its cohesin. Using this approach, the ScaG cohesin was able to bind to the ScaA dockerin (Figure 1 and Figure 2B), suggesting an adaptor role for this scaffoldin between ScaK and the enzyme-bearing scaffoldin ScaA. A scheme illustrating the interactions between ScaK and the cellulosomal elements is presented in Figure 3. Consequently, the ScaG cohesin is now considered a Group-2 cohesin, and the ScaK cohesin and dockerins of ScaA and Prot3939 belong to the Group-1 interacting modules.

ScaF exhibits the same modular architecture as ScaG (Figure 1), but with a longer linker region at the N-terminus of the protein. Similar to ScaG, when the cohesin and dockerin modules were expressed separately, only the dockerin was active and exhibited similar binding abilities as the ScaG dockerin (Ben David et al., 2015). Similar to ScaK and ScaG, the expression of the full-length scaffoldin revived

the cohesin activity, and specific interaction with the ScaG dockerin was observed (Supplemental Figure S2). As ScaG and ScaF dockerins exhibited the same binding affinities and both can bind directly to the ScaE cohesin, it is not clear why the bacterium would produce and assemble an additional adaptor scaffoldin (i.e., ScaF) to mediate between ScaG and ScaE (via ScaJ) (Supplemental Figure S3). In this context, ScaF could perhaps serve as an extender to increase the overall length of the cellulosome in order to avoid steric hindrance or to access more distant substrates.

Lysozyme activity.

The enzymatic activity was monitored by decrease in turbidity of the cultures. The lysozyme module of ScaK was active on *E. coli* cells between pH 3.5 and 5.5 with a pH optimum of 5 (Figure 4A). The activity of the enzyme was lost completely at pH 6 and higher. The protein was stable between 30 and 60°C for 48 h. At 70°C, the lysozyme retained its full activity after 3 h of incubation and was 54% active after 24 h of incubation. After 48 h of incubation at this temperature, the enzyme was still 30% active. At 80°C, the enzyme was more rapidly degraded, but was still 20% active after 48 h of incubation (Figure 4B). ScaK was active on *E. coli* cells from 2 to 45°C. Enzymatic activity increased with the temperature as monitored by the decrease in turbidity and viable cell count (Figure 4C). In addition, the enzyme was active from 2 to 85°C on purified peptidoglycans from *Bacillus subtilis* and *Staphylococcus aureus* along the entire temperature range with moderate enhancement of activity with increasing temperature (Figure 4D).

The lytic activity of ScaK was tested against a large number of strains that colonize the human gut and additional bacteria (Table 2). The lysozyme was found to be inactive against the parent *R. champanellensis* cells but active against several Lactobacillus strains, *E. coli*, *Enterococcus faecalis*, *Listeria monocytogenes* and *Streptococcus pneumoniae*. *Clostridium difficile* was degraded after long incubation periods. Growth of *E. coli* and *L. plantarum* was inhibited by the presence of the lysozyme, as demonstrated by inhibition zones around disks containing the enzyme during growth on plates (Supplemental Figure S4).

The potential protective role of the bacterial capsule against bacterial cell lysis was tested by incubating the lysozyme with *E. coli* strains producing a capsule (5911 and Nissle strains), and no lytic action was observed. In addition, *Bacteroides thetaiotaomicron*, was tested using both the wild-type strain and a mutant lacking any

capsule (Rogers et al., 2013), and in both cases no lysis was observed (Table 2).

Expression of ScaK by *R. champanellensis*.

ScaK was detected by proteomic analysis in supernatant fluids of *R. champanellensis* cultures grown on cellobiose as the sole carbon source (score of 9.45 and % coverage of 9.23, p-value<0.01), suggesting that it is indeed incorporated in the cellulosomal complex and participates in bacterial lignocellulose degradation as a possible inhibitor of other competing or deleterious bacteria which inhabit the human gastrointestinal tract.

Discussion

The ScaK scaffoldin of *Ruminococcus champanellensis* contains the first cellulosome-associated GH25 known to date. The enzyme is active at extremes of temperature and stable for long incubation periods at elevated temperatures. These characteristics could therefore render the ScaK enzyme a suitable candidate for industrial applications, for example, as an antimicrobial agent in the food industry (Datta et al., 2008; Callewaert et al., 2011; Aminlari et al., 2014) and may also be considered as a therapeutic agent in humans (Pastagia et al., 2013).

Curiously, ruminococci seem to carry numerous non-cellulosomal GH25 genes – nine in *R. flavefaciens* FD1, five in *R. bicirculans* 80/3, five in *R. albus* 7, one in *R. bromii* and three in *R. champanellensis* 18P13 (in addition to the ScaK gene). Since genomic analysis has indicated that prophage DNA (encoding lysozymes) is rather common in this group of bacteria (Berg Miller et al., 2012; Wegmann et al., 2014), we analyzed the flanking regions of the ScaK gene for the presence of phage genes, such as holins (Supplemental Table 1). In the absence of such genes, bacteriophage origin would thus be improbable. Therefore, the association of the cohesin module and a GH25 gene only with the *R. champanellensis* GH25 raises the question of a biological role for this scaffoldin in its cellulosomal complex.

The production of ScaK, ScaG and ScaF as intact proteins revived the binding activity of their lone cohesins towards the specified dockerins, suggesting that the functional status and/or structural stability of the cohesin modules of these scaffoldins is dependent on the full protein architecture. We could thus elucidate their dockerin

specificities and therefore complete the proposed architecture of the *R. champanellensis* cellulosome system. The results indicate that cell-free cellulosomes can be formed between ScaK that interacts with ScaG, which in turn interacts with ScaA that harbors the enzymes either directly or through ScaC and ScaD adaptors. This type of cellulosome could thus be targeting plant-derived lignocellulosic materials located at a distance from the cell.

The ScaK cohesin was also found to interact with the dockerin of protein 3939. This very large protein has an estimated molecular weight of 308 kDa, and annotation of its sequence has revealed five predicted Fn3 (fibronectin type III) and two PKD (polycystic kidney disease) domains. The Fn3 domains are relatively common components in celluloytic bacteria, yet their function is not completely understood. Several studies suggested that these domains can mediate protein assembly, adhesion to carbohydrate substrates and/or bacterial cell surfaces (which is in accordance with lysozyme activity). Alternatively, Fn3 domains have been suggested to play a role as flexible peptide linkers or to facilitate the solubility of large protein complexes (Devillard et al., 2004; Alahuhta et al., 2010). In addition, PKD domains have also been found to be involved in protein-protein and/or protein-carbohydrate interactions (Lohning et al., 1996). Therefore, we can assume that protein 3939 may have an important, but largely undefined role in carbohydrate degradation, which would benefit the bacterium in general and would justify the expression and secretion of such a large protein. The dockerin of protein 3939 was previously reported to also interact with ScaE that is anchored to the bacterial cell wall (Ben David et al., 2015).

It is also of note that other putative lysozymes can be encoded by GH23-, GH24- and GH73-containing genes in other bacterial genomes. Interestingly, the sole dockerin of the *R. bicirculans* genome was associated with a GH73 catalytic domain (Wegmann et al., 2014), suggesting a similar mechanism and role for the lysozyme in this bacterium.

It is plausible that the GH25 lysozyme has a defensive role against other carbohydrate-degrading bacterial competitors by targeting and effecting the lysis of bacterial cells in the vicinity that would compete for the enzymatic degradation products. In nature, *R. champanellensis* and other specialized fiber-degrading bacteria are prone to exploitation by cheating microbes that utilize the fiber-released soluble sugars, taking advantage of the bacterial fiber-degrading machineries carried without

paying the fitness cost (Berlemont and Martiny, 2013). It is therefore reasonable to assume that the fiber degraders will develop defense mechanisms protecting them from such exploitation. In this sense, the GH25 lysozyme exhibits an efficient selective tactic, as it does not affect the parent *R. champanellensis* cell itself, but lyses other gut microbial cells (Table 2).

The bacterial spectrum of susceptibility to ScaK is quite heterogeneous, whereby some Gram-positive (*Lactobacillus* species, *Enterococcus faecalis*, *Listeria monocytogenes, Streptococcus pneumoniae* and *Clostridium difficile*) and Gram-negative (*E. coli*) bacteria were lysed. Our results initially suggested that ScaK specifically degraded peptidoglycans that contain meso-diaminopimelate (m-DAP) residues in the peptidoglycan structure (Schleifer and Kandler, 1972; Humann and Lenz, 2009), since all the strains that were herein susceptible to ScaK lytic action contained m-DAP. However, since the isolated purified peptidoglycan of *S. aureus,* which contains D-alanine residue and not m-DAP, was degraded, this hypothesis was thus invalidated.

Bacterial defense mechanisms against lysozyme activity are diverse and include the production of enzyme inhibitors or modification of the peptidoglycan (Callewaert et al., 2012), as well as the production of bacterial capsules (Fouet and Mesnage, 2002). We thus investigated the role of the bacterial capsule as a possible protection against the lysozyme action by testing *E. coli* strains with and without capsules. In the case of the two encapsulated strains of *E. coli*, i.e., Nissle and 5911, the capsule indeed conferred resistance to ScaK lytic action. It should also be noted that capsule expression is highly controlled and regulated (Torres-Cabassa and Gottesman, 1987; Gottesman and Stout, 1991; Sledjeski and Gottesman, 1996) and that four different types of bacterial capsules are described to date in *E. coli* (Whitfield and Roberts, 1999). The strains tested herein belong to group 2 capsules (capsular gene K5 and K12 for Nissle and 5911 strains, respectively). Therefore, other groups of capsules may confer resistance to the lytic action of ScaK or not, depending also on the growth conditions and extent of capsule expression. We also investigated the capsular protective role with two different strains of *Bacteroides thetaiotaomicron* (Shah, 2013). The two strains tested were the wild type strain and a mutant lacking any capsule. In both cases, no lysis was observed. Consequently, together with the non-susceptible Gram-negative bacteria tested herein, the outer membrane may act as an impermeable barrier for small molecules thereby protecting the peptidoglycan layer

from the lytic action of the lysin (Briers and Lavigne, 2015). Nevertheless, some endolysins have been reported to cross the outer membrane and lyse the bacteria (Lai et al., 2011; Lood et al., 2015). This ability could reflect highly positively charged N- or C-terminal domains in their protein sequence, which enable the lysins to bind to the anionic outer membrane and access their peptidoglycan substrate (Lai et al., 2011). In our case, we could not identify a similar domain in ScaK that could account for the lysis of the Gram-negative acapsulated strains of *E. coli* (*BL21* and *5911*).

In conclusion, we identified the presence of a non-autolytic lysozyme in the *R. champanellensis* cellulosome system. The production of this cell-free cellulosome would represent a strategy to hydrolyze lignocellulose while repelling eventual food competitors or cheaters. The fact that this lysozyme activity is associated with glycoside hydrolases in a single cell-free cellulosome complex suggests a broader role for cellulosomal complexes that would not be restricted to plant cell wall deconstruction.

Experimental Procedures

Cloning. Scaffoldins ScaK, ScaG and ScaF were cloned from *R. champanellensis* genomic DNA using Phusion High Fidelity DNA polymerase F530-S (New England Biolabs, Inc) and the following primers. For ScaK amplification, the primer pair 5'-ttactaCCATGGcacaccatcaccatcaccatgcagatcagactgtacagac-3' and 5'-ttactaCTCGAGttaaaacccattaaatccgt-3' was used, for ScaG, 5'-tactgaCCATGGcacaccatcaccatcaccatcagaccatgcagccggcggc-3' and 5'-tacttaCTCGAGtcaaccgagcaggtcatccc-3' and for ScaF 5'-tactgaCCATGGcacaccatcaccatcaccatgcatccggattgacctacag-3' and 5'-tacgatCTCGAGtcaccattgcggattcggatc-3'. NcoI and XhoI (restriction sites in uppercase). Fastdigest enzymes (Thermo scientific, USA) were incubated with the PCR products before their ligation into linearized pET28a using T4 DNA ligase (Fermentas UAB, Vilnius, Lithuania). PCR products were purified using a HiYield™ Gel/PCR Fragments Extraction Kit (Real Biotech Corporation, RBC, Taiwan), and plasmids were extracted using Qiagen miniprep kit (Netherlands). Competent *E. coli* XL1 cells were used for plasmid transformation.

The full list of fused dockerins used in this article is given in Table 1.

Recombinant protein expression and purification. *E. coli* BL21 (DE3) cells were transformed with the desired plasmid and plated onto LB-kanamycin plates. The cells producing ScaK, ScaG and ScaF were grown in 500 ml LB (Luria Broth) and 2 mM $CaCl_2$ at 37°C until A_{600}≈0.8-1. The cells were induced by adding 0.1 mM (final concentration) of isopropyl-1-thio-β-D-galactoside (IPTG) (Fermentas UAB Vilnius, Lithuania), and cell growth was continued at 16°C overnight. Cells were harvested by centrifugation at 5000 rpm for 5 min. Pelleted cells were resuspended in 1 ml TBS (Tris-buffered saline, 137 mM NaCl, 2.7 mM KCL, 25 mM Tris-HCl, pH 7.4). Xyn-Doc proteins were expressed as described previously (Ben David et al., 2015; Morais et al., 2015).

His-tagged proteins (scaffoldins and Xyn-Doc) were purified on a Ni-NTA column (Qiagen), as reported earlier (Caspi et al., 2006).

Purity of the recombinant proteins was tested by SDS-PAGE on 10% acrylamide gels, and protein concentration was estimated by absorbance (280 nm), based on the known amino acid composition of the protein, using the Protparam tool (Gasteiger et al., 2005). Proteins were stored in 50% (v/v) glycerol at -20°C.

Affinity-based ELISA. The matching fusion-protein procedure of Barak et al (Barak et al., 2005; Caspi et al., 2006) was followed to determine cohesin-dockerin specificity of interaction. Scaffoldins were immobilized on the plate at a concentration of 1 μg/ ml (100 μl/well) in 0.1 M sodium carbonate (pH 9) and incubated at 4°C overnight. The following steps were performed at room temperature for 1 h with all reagents at a volume of 100 μl/well with a washing step (300 μl/well blocking buffer without BSA) repeated three times after each step. The coating solution was discarded, and blocking buffer (TBS, 10 mM $CaCl_2$, 0.05% Tween 20, 2% BSA) was added. The blocking buffer was discarded, and the desired representative Xyn-Doc(s) (Xyn-DocA, Xyn-DocB, Xyn-DocC, Xyn-DocD, Xyn-DocF, Xyn-DocG, Xyn-DocH, Xyn-DocJ, Xyn-Doc3939, Xyn-Doc48, Xyn-Doc9b, Xyn-Doc3550), diluted to concentrations of 0.1, 1, 10 and 100 ng/ml in blocking buffer, were added. Rabbit anti-xylanase antibody (diluted 1:10000) was used as the primary antibody preparation, and secondary antibody preparation was HRP-labeled anti-rabbit antibody diluted 1:10000 in blocking buffer. Substrate-Chromogen TMB (Dako, Agilent Technologies, USA) was added at 100 μl/well, and the reaction was carried out for 2 min before color formation was terminated upon addition of 1 M H_2SO_4 (50

355 µl/well), and the absorbance was measured at 450 nm using a tunable microplate
356 reader.

357 **Enzymatic activity assay.** All assays were performed at least twice in triplicate.
358 ScaK enzymatic activity was monitored using the turbidimetric method (Shugar,
359 1952; Diez-Martinez et al., 2015) with modifications. The enzyme was applied at a
360 concentration of 50 µg/ ml, and *E. coli* BL21 at OD_{600nm}= 1 was used as a substrate
361 for examining pH and temperature effects on the enzyme. After 30 min incubation
362 time, decreases in optical densities were read at 600 nm after centrifuging 2 min at
363 1000 rpm (60 x g) to clear cell debris. At this centrifugal speed, less than 10% of the
364 bacterial cells precipitate, for short time periods (2 min) as can be observed in
365 Supplemental Figure S5A and S5B. Without the centrifugation step, cell debris (that
366 precipitate only gradually over extended time periods) can float and OD
367 measurements can be less accurate. Controls without enzyme were also submitted to
368 the centrifugal step so that the 10% precipitation of the bacterial cells does not affect
369 the results. Supplemental Figure S5C presents the effect of temperature on lytic
370 activity after 1 h incubation without the centrifugation step, and the results tend to be
371 similar to those presented in Figure 4C with the centrifugation step.

372 The pH optimum was determined by using acetate buffer ranging from pH 3.5
373 to 6.5 and MOPS (3-(N-morpholino)propanesulfonic acid) from pH 6.5 to 9. The
374 enzyme was incubated at 37°C for 15 min. Temperature optima were tested at pH 5
375 (50 mM acetate buffer) between temperatures ranging from 2 to 45°C, and reactions
376 were terminated after 30-min incubation. We used a viability assay (Diez-Martinez et
377 al., 2015) to follow the temperature effect on ScaK lytic action. Measurement of
378 viable *E. coli* cells was carried out in LB agar plates after 30-min incubation at each
379 temperature. For each sample, a 10-fold dilution series was prepared in LB, and 100
380 µl of each dilution was plated. Colonies were counted after overnight incubation at
381 37°C.

382 The susceptibility of the peptidoglycans from *B. subtilis* and *S. aureus* (Sigma-
383 Aldrich, Israel) to lysozyme was analyzed with a turbidometric assay (Bera et al.,
384 2005; Wang et al., 2009). The peptidoglycans were diluted to 0.5 mg/ml in double
385 distilled water, and the lysozyme was added to a concentration of 50 µg/ ml at pH 5
386 (50 mM acetate buffer). The absorbance at 450 nm was monitored after 30 min of

incubation at temperatures ranging from 2 to 85°C.

Stability of the protein was tested for 30 min at 37°C after incubation for 1, 3, 24 and 48 h at 30, 40, 50, 60, 70 and 80°C.

Bacterial strains and growth medium. The bacterial species tested in this study are listed in Table 2. All the strains were cultured at 37°C (anaerobic strains were grown under anaerobic conditions) and tested for their sensitivity to ScaK *in vitro* as described above (at 1 h incubation time). Certain strains listed in Table 2 were held in stock by the authors S.H. Duncan and H.J. Flint (U. of Aberdeen). The 18 cultures provided for testing for ScaK lytic activity were *Bifidobacterium adolescentis* L2-32, *Collinsella aerofaciens* DSM 3979, *Enterococcus faecalis* JH2-2, *Eubacterium hallii* L2-7 (DSM 17630), *Anaerostipes hadrus* Ss2/1, *Blautia obeum* A2-162, *Eubacterium rectale* A1-86 (DSM 17629), *Roseburia faecis* M72/1 (DSM 16840), *Lachnospiraceae* sp. nov. M62/1, *Lactobacillus reuteri* Ca6, *Ruminococcus champanellensis* 18P13 (DSM 18848), *Ruminococcus bicirculans* 80/3, *Ruminococcus bromii* L2-63, *Eubacterium siraeum* 70/3, *Faecalibacterium prausnitzii* A2-165 (DSM 17677), *Ruminococcus flavefaciens* 17, *Ruminococcus albus* SY3 and *Streptococcus gordonii* DL-1. Those available from Deutsche Sammlung von Mikroorganismen und Zellkulturen (DSMZ), Germany) are indicated by DSM numbers in brackets. Cultures were prepared by growing on M2GSC medium (Miyazaki et al., 1997) for approximately 24 h under CO_2 prior to testing for ScaK lysis. *E. coli* BL21 and Nissle, *Bacillus subtilis* NCIB 3610 and PY79 strains, *Acinetobacter baumanii* ATCC 17978, *Listeria monocytogenes* 10403S and *Vibrio cholerae* TRH7000 were cultured in LB. Bacteroides thetaiotaomicron ATCC 29148 and ΔCPS (Cameron et al., 2014) were cultured in TYG (Holdeman et al., 1977). *Lactobacillus plantarum* WCFS1, *Lactobacillus pentosus* DSM 20314, *Lactobacillus reuteri* Ca6 and *Lactobacillus rhamnosus* GG were cultured in MRS. *Lactococcus lactis* MG5267 and Z3000 strains were cultured in M17. *Clostridium difficile* VPI 10463 was cultured in BHIS (Sorg and Dineen, 2009). *Clostridium thermocellum* DSM 1313 and *Clostridium clarifavum* DSM 19732 were cultured in GS-2 medium. *Ruminococcus champanellensis* 18P13 was cultured in M2 medium. *Streptococcus pneumoniae* R6 was grown in Todd Hewitt broth supplemented with 5% yeast extract (Updyke and Nickle, 1954).

E. coli strain 5911 was grown for 3 h in LB, and capsule expression was

induced by addition of 15% sucrose (Sledjeski and Gottesman, 1996). The cells were then grown overnight at 37°C and incubated at room temperature for a week.

Bacterial cells were tested by the turbidimetric assay as described above.

Inhibition test. *E. coli* BL21 and *L. plantarum* WCFS1 cells were spread on the entire surface of LB or MRS plates prepared at pH 5. Sterile filter paper disks (catalogue number 74146, Sigma Aldrich, Israel) containing either sterile water or 2 g/l ScaK were placed in the middle of the plates, and the plates were incubated overnight at 37°C.

Label free LC MS-MS analysis. Proteolysis and mass spectrophometry analysis of *R. champanellensis* culture supernatants, grown on cellobiose as a carbon source (Lopez-Siles et al., 2012; Morais et al., 2015), were performed as described by Artzi (Artzi et al., 2015).

Acknowledgements

This research was supported by a grant to EAB, NMK and ECM from the United States-Israel Binational Science Foundation (BSF), Jerusalem, Israel and by a grant (No. 1349) to EAB from the Israel Science Foundation (ISF). Additional support was obtained from the establishment of an Israeli Center of Research Excellence (I-CORE Center No. 152/11) managed by the Israel Science Foundation. The authors also appreciate the support of the European Union, Area NMP.2013.1.1-2: Self-assembly of naturally occurring nanosystems: CellulosomePlus Project number: 604530. HJF and SHD acknowledge financial support from the Scottish Government Rural and Environmental Sciences and Analytical Services (SG-RESAS) and from BBSRC grant no BB/L009951/1. EAB is the incumbent of The Maynard I. and Elaine Wishner Chair of Bio-organic Chemistry.

Conflict of Interest

The authors declare no conflict of interest

Table 1: List of the *R. champanellensis* Xyn-fused dockerin proteins used in this study. Name and modular architecture of the original scaffoldin or protein are given. Abbreviations: Xyn, XynT6 from the *G. stearothermophilus*; SIGN, signal peptide; Doc, dockerin; Coh, cohesin; GH, glycoside hydrolase; SGNH, lipases or esterases; Fn3, fibronectin type III; PKD, polycystic kidney disease; UNK, X, unknown.
The numbers for proteins 3550 and 3939 refer to the last four digits of the respective full GI number (i.e. 29154XXXX).

Fused dockerin	Parent scaffoldin/protein	Modular architecture	Dockerin group
Xyn-DocA	ScaA	SIGN X Coh Coh **Doc**	2
Xyn-DocB	ScaB	SIGN Coh Coh Coh Coh Coh Coh Coh X **Doc**	1
Xyn-DocC	ScaC	SIGN Coh UNK **Doc**	2
Xyn-DocD	ScaD	SIGN Coh **Doc**	2
Xyn-DocF	ScaF	SIGN Coh **Doc**	1
Xyn-DocG	ScaG	SIGN Coh **Doc**	1
Xyn-DocH	ScaH	SIGN SGNH Coh **Doc**	1
Xyn-DocJ	ScaJ	SIGN Coh Coh Coh **Doc**	1
Xyn-Doc3939	gi:291543939	SIGN Fn3 PKD Fn3 Fn3 Fn3 Fn3 PKD **Doc**	1
Xyn-Doc48	Cel48A	SIGN GH48A **Doc**	2
Xyn-Doc9B	GH9B	SIGN CBM4 Fn3 GH9B **Doc** GH16A	3-4
Xyn-Doc3550	gi:291543550	UNK **Doc**	3-4

459
460 Table 2: Bacterial strains tested for ScaK lytic action. Enzymatic activity was
461 monitored by decrease in turbidimetry in cell cultures at 600 nm, from the beginning
462 $OD_{T=0}$ to the end of the reaction $OD_{T=1h}$. Classification of the Firmicutes based on
463 Ludwig et al (Ludwig et al., 2009).
464 [a] grown with sucrose
465

Bacterial phyla/ (family)/*species*/strain	**Gram**	**$OD_{T=0}$**	**$OD_{T=1h}$**	**ScaK lytic action**
Actinobacteria				
(Bifidobacteriaceae)				
Bifidobacterium adolescentis L2-32	+	**0.132**	**0.124**	–
(Coriobacteriaceae)				
Collinsella aerofaciens DSM 3979	+	**0.094**	**0.095**	–
Firmicutes				
(Bacillacae)				
Bacillus subtilis NCIB 3610	+	**1.200**	**1.195**	–
Bacillus subtilis PY79	+	**1.220**	**1.199**	–
(Enterococcaceae)				
Enterococcus faecalis JH2-2	+	**0.299**	**0.210**	+
(Lachnospiraceae)				
Eubacterium hallii L2-7	+	**0.085**	**0.074**	–
Eubacterium rectale A1-86 (DSM17629)	+	**0.925**	**0.884**	–
Anaerostipes hadrus SS2/1	+	**1.100**	**1.029**	–
Lachnospiraceae sp. nov. M62/1	+	**0.085**	**0.088**	–
Blautia obeum A2-162	+	**1.030**	**0.984**	–
Roseburia faecis M72/1	+	**0.862**	**0.856**	–
(Lactobacillaceae)				
Lactobacillus plantarum WCFS1	+	**1.840**	**0.368**	+
Lactobacillus pentosus DSM 20314	+	**1.560**	**0.267**	+
Lactobacillus reuteri Ca6	+	**0.210**	**0.214**	–
Lactobacillus rhamnosus GG	+	**1.952**	**0.341**	+
(Listeriaceae)				
Listeria monocytogenes 10403S	+	**1.194**	**0.467**	+
(Peptostreptococcaceae)				
Clostridium difficile VPI 10463	+	**0.470**	**0.418 (T=4h)**	±
(Ruminococcaceae)				
Ruminococcus champanellensis 18P13	+	**1.130**	**1.259**	–

Ruminococcus bicirculans 80/3	+	**0.459**	**0.444**	–
Ruminococcus bromii L2-63	+	**0.382**	**0.361**	–
Eubacterium siraeum 70/3	+	**0.437**	**0.422**	–
Faecalibacterium prausnitzii A2-165	+	**0.336**	**0.335**	–
Ruminococcus flavefaciens 17	+	**0.331**	**0.330**	–
Ruminococcus albus SY3	+	**0.689**	**0.665**	–
Clostridium clariflavum DSM 19732	+	**1.345**	**1.322**	–
Clostridium thermocellum DSM 1313	+	**1.202**	**1.197**	–
(Streptococcaceae)				
Lactococcus lactis MG5267	+	**1.500**	**1.501**	–
Lactococcus lactis Z3000	+	**1.500**	**1.499**	–
Streptococcus gordonii DL-1	+	**0.109**	**0.100**	–
Streptococcus pneumoniae R6	+	**0.480**	**0.051**	+
Bacteroidetes				
(Bacteroideaceae)				
Bacteroides thetaiotaomicron ATCC 29148	–	**1.573**	**1.559**	–
Bacteroides thetaiotaomicron ΔCPS	–	**1.567**	**1.509**	–
Proteobacteria				
(Enterobacteriaceae)				
Escherichia coli BL21	–	**1.462**	**0.206**	+
Escherichia coli 5911 (K12)	–	**1.500**	**0.190**	+
Escherichia coli 5911 (K12)[a]	–	**1.423**	**1.360**	–
Escherichia coli Nissle	–	**1.692**	**1.666**	–
(Moraxellaceae)				
Acinetobacter baumanii ATCC 17978	–	**0.689**	**0.648**	–
(Vibrionaceae)				
Vibrio cholera TRH7000	–	**0.656**	**0.619**	–

466

Figure legends

Figure 1: Schematic representation of the cohesin-bearing scaffoldin proteins in *R. champanellensis* based on the respective genome sequences. SGNH, hydrolase-type esterase domain (IPR013830); GH25, a putative GH25-family module sharing similarity to lysozyme. Specific interactions according to sequence alignment and biochemically characterized cohesin/dockerin interactions are color-coded. Shaded colors indicate that the designated cohesins or dockerins exhibit more selective interactions with only some of their Group 1 or Group 2 counterparts.

Figure 2: Newly discovered dockerin-binding profiles of *R. champanellensis* ScaK and ScaG cohesins measured by affinity ELISA (**A**) ELISA experiments demonstrating different interaction specificities between the ScaK cohesin and selected scaffoldin- and enzyme-borne dockerins. ScaK interacted with DocG and Doc3939 (**B**) ELISA experiments demonstrating different interaction specificities between the ScaG cohesin and selected scaffoldin- and enzyme-borne dockerins. ScaG interacted exclusively with DocA. Error bars indicate the standard deviation from the mean of triplicate samples (ELISA). The experiments were performed three times.

Figure 3: Proposed cell-free cellulosome complexes involving ScaK in *R. champanellensis*. Different types of cohesin-dockerin interactions are color-coded. The ScaK cohesin binds selectively to the dockerins of ScaG and Prot3939 and not to other Group 1 dockerins. Similarly, the ScaG cohesin appears to be very selective in its binding to the ScaA dockerin, and fails to bind other Group 2 dockerins.

Figure 4: Characterization of recombinant *R. champanellensis* ScaK. (A) Effect of pH on lysozyme activity after 15 min incubation. (B) Thermostability of ScaK-derived lysozyme activity at different temperatures, following the heat-shock, the enzymatic activity was measured at pH 5 after 30 min incubation at 37°C. (C) Effect of temperature on lysozyme activity on *E. coli* cells at pH 5 after 30 min incubation, solid line representing the decrease in OD at 600 nm and dashed line, the viability of the cells (in cfu/ml) with the control counting $1.6.10^{12}$ cfu/ml. (D) Effect of temperature on lysozyme activity on the peptidoglycans of *B. subtilis* (blue line) and *S. aureus* (red line) at pH 5 after 30 min incubation. Enzymatic reactions, performed using the modified turbidimetric method were repeated in triplicate, and standard deviations are indicated.

Supplemental Figures

Supplemental Figure S1: Purity of the recombinant scaffoldins after Ni-NTA purification as assessed by SDS-PAGE gels. A. ScaK, molecular weight 52326 Da (10% acrylamide), B. ScaG, molecular weight 29510 Da (12% acrylamide) and C. ScaF, molecular weight 25633 Da (12% acrylamide).

Supplemental Figure S2: *R. champanellensis* ScaF interactions measured by ELISA with selected dockerins. The cohesin only binds to the dockerin of ScaG. Error bars indicate the standard deviation from the mean of triplicate (ELISA) from three experiments.

Supplemental Figure S3: Proposed cell-bound cellulosome complexes involving ScaG and ScaF in *R. champanellensis*. Different types of cohesin-dockerin interactions are color-coded. The ScaG and ScaF dockerins are selective for the cohesins of ScaE and ScaJ1. The ScaG dockerin also binds selectively to the ScaF cohesin, but the ScaF cohesin fails to bind to its own dockerin. The ScaG cohesin appears to be very selective in its binding to the ScaA dockerin and fails to bind other Group 2 dockerins.

Supplemental Figure S4: Inhibition of *L. plantarum* (A) and *E. coli* (B) growth by the presence of the GH25 lysozyme on disks (2 g/l). The cells were grown on MRS and LB plates prepared at pH 5. Inhibition zones are marked with red arrows.

Supplemental Figure S5: Effect of time on the precipitation of bacterial cells *L. plantarum* (A) and *E. coli* (B) at a centrifugal speed of 1000 rpm (60 x g). (C) Effect of temperature on lysozyme activity on *E. coli* cells after 1 h incubation at pH 5 without the centrifugation step.

References

Alahuhta, M., Xu, Q., Brunecky, R., Adney, W.S., Ding, S.Y., Himmel, M.E., and Lunin, V.V. (2010) Structure of a fibronectin type III-like module from *Clostridium thermocellum*. *Acta Crystallogr Sect F Struct Biol Cryst Commun* **66**: 878-880.

Aminlari, L., Hashemi, M.M., and Aminlari, M. (2014) Modified lysozymes as novel broad spectrum natural antimicrobial agents in foods. *Journal of food science* **79**: R1077-1090.

Artzi, L., Morag, E., Barak, Y., Lamed, R., and Bayer, E.A. (2015) *Clostridium clariflavum*: Key Cellulosome Players Are Revealed by Proteomic Analysis. *mBio* **6**: e00411-00415.

Barak, Y., Handelsman, T., Nakar, D., Mechaly, A., Lamed, R., Shoham, Y., and Bayer, E.A. (2005) Matching fusion protein systems for affinity analysis of two interacting families of proteins: the cohesin-dockerin interaction. *J Mol Recognit* **18**: 491-501.

Bayer, E.A., Lamed, R., and Himmel, M.E. (2007) The potential of cellulases and cellulosomes for cellulosic waste management. *Current opinion in biotechnology* **18**: 237-245.

Bayer, E.A., Belaich, J.-P., Shoham, Y., and Lamed, R. (2004) The cellulosomes: Multi-enzyme machines for degradation of plant cell wall polysaccharides. *Annu Rev Microbiol* **58**: 521-554.

Ben David, Y., Dassa, B., Borovok, I., Lamed, R., Koropatkin, N.M., Martens, E.C. et al. (2015) Ruminococcal cellulosome systems from rumen to human. *Environ Microbiol* **17**: 3407–3426.

Bera, A., Herbert, S., Jakob, A., Vollmer, W., and Gotz, F. (2005) Why are pathogenic staphylococci so lysozyme resistant? The peptidoglycan O-acetyltransferase OatA is the major determinant for lysozyme resistance of *Staphylococcus aureus*. *Mol Microbiol* **55**: 778-787.

Berg Miller, M.E., Yeoman, C.J., Chia, N., Tringe, S.G., Angly, F.E., Edwards, R.A. et al. (2012) Phage-bacteria relationships and CRISPR elements revealed by a metagenomic survey of the rumen microbiome. *Environ Microbiol* **14**: 207-227.

Berlemont, R., and Martiny, A.C. (2013) Phylogenetic distribution of potential cellulases in bacteria. *Applied and environmental microbiology* **79**: 1545-1554.

Briers, Y., and Lavigne, R. (2015) Breaking barriers: expansion of the use of endolysins as novel antibacterials against Gram-negative bacteria. *Future microbiology* **10**: 377-390.

Callewaert, L., Walmagh, M., Michiels, C.W., and Lavigne, R. (2011) Food applications of bacterial cell wall hydrolases. *Current opinion in biotechnology* **22**: 164-171.

Callewaert, L., Van Herreweghe, J.M., Vanderkelen, L., Leysen, S., Voet, A., and Michiels, C.W. (2012) Guards of the great wall: bacterial lysozyme inhibitors. *Trends in microbiology* **20**: 501-510.

Cameron, E.A., Kwiatkowski, K.J., Lee, B.H., Hamaker, B.R., Koropatkin, N.M., and Martens, E.C. (2014) Multifunctional nutrient-binding proteins adapt human symbiotic bacteria for glycan competition in the gut by separately promoting enhanced sensing and catalysis. *mBio* **5**: e01441-01414.

Caspi, J., Irwin, D., Lamed, R., Shoham, Y., Fierobe, H.-P., Wilson, D.B., and Bayer, E.A. (2006) *Thermobifida fusca* family-6 cellulases as potential designer cellulosome components. *Biocat Biotransform* **24**: 3-12.

Chassard, C., Delmas, E., Robert, C., Lawson, P.A., and Bernalier-Donadille, A. (2012) *Ruminococcus champanellensis sp. nov*., a cellulose-degrading bacterium from human gut microbiota. *Int J Syst Evol Microbiol* **62**: 138-143.

Claverys, J.P., Martin, B., and Havarstein, L.S. (2007) Competence-induced fratricide in streptococci. *Mol Microbiol* **64**: 1423-1433.

Datta, S., Janes, M.E., Xue, Q.G., Losso, J., and La Peyre, J.F. (2008) Control of *Listeria monocytogenes* and *Salmonella anatum* on the surface of smoked salmon coated with calcium alginate coating containing oyster lysozyme and nisin. *Journal of food science* **73**: M67-71.

Devillard, E., Goodheart, D.B., Karnati, S.K., Bayer, E.A., Lamed, R., Miron, J. et al. (2004) *Ruminococcus albus* 8 mutants defective in cellulose degradation are deficient in two processive endocellulases, Cel48A and Cel9B, both of which possess a novel modular architecture. *Journal of bacteriology* **186**: 136-145.

Diez-Martinez, R., De Paz, H.D., Garcia-Fernandez, E., Bustamante, N., Euler, C.W., Fischetti, V.A. et al. (2015) A novel chimeric phage lysin with high in vitro and in vivo bactericidal activity against *Streptococcus pneumoniae*. *The Journal of antimicrobial chemotherapy* **70**: 1763-1773.

Eldholm, V., Johnsborg, O., Haugen, K., Ohnstad, H.S., and Havarstein, L.S. (2009) Fratricide in *Streptococcus pneumoniae*: contributions and role of the cell wall hydrolases CbpD, LytA and LytC. *Microbiology* **155**: 2223-2234.

Fouet, A., and Mesnage, S. (2002) *Bacillus anthracis* cell envelope components. In *Anthrax*. Koehler, T.M. (ed). Berlin, Heidelberg: Springer Berlin Heidelberg, pp. 87-113.

Gasteiger, E., Hoogland, C., Gattiker, A., Duvaud, S., Wilkins, M.R., Appel, R.D., and Bairoch, A. (2005) Protein Identification and Analysis Tools on the ExPASy Server. In *The Proteomics Protocols Handbook*. Walker, J.M. (ed). Totowa, NJ Humana Press, pp. 571-607.

Gottesman, S., and Stout, V. (1991) Regulation of capsular polysaccharide synthesis in *Escherichia coli* K12. *Mol Microbiol* **5**: 1599-1606.

Himmel, M., Xu, Q., Luo, Y., Ding, S., Lamed, R., and Bayer, E. (2010) Microbial enzyme systems for biomass conversion: Emerging paradigms. *Biofuels* **1**: 323-341.

Holdeman, L.V., Cato, E.D., and Moore, W.E.C. (1977) *Anaerobe Laboratory Manual*. Blacksburg, VA: Virginia Polytechnic Institute and State University Anaerobe Laboratory.

Humann, J., and Lenz, L.L. (2009) Bacterial peptidoglycan degrading enzymes and their impact on host muropeptide detection. *Journal of innate immunity* **1**: 88-97.

Lai, M.J., Lin, N.T., Hu, A., Soo, P.C., Chen, L.K., Chen, L.H., and Chang, K.C. (2011) Antibacterial activity of *Acinetobacter baumannii* phage varphiAB2 endolysin (LysAB2) against both gram-positive and gram-negative bacteria. *Appl Microbiol Biotechnol* **90**: 529-539.

Lohning, C., Pohlschmidt, M., Glucksmann-Kuis, M.A., Duyk, G., Bork, P., Schneider, M.O. et al. (1996) Structural motifs of the PKD1 protein. *Nephrology, dialysis, transplantation : official publication of the European Dialysis and Transplant Association - European Renal Association* **11 Suppl 6**: 2-4.

Lood, R., Winer, B.Y., Pelzek, A.J., Diez-Martinez, R., Thandar, M., Euler, C.W. et al. (2015) Novel phage lysin capable of killing the multidrug-resistant gram-negative bacterium *Acinetobacter baumannii* in a mouse bacteremia model. *Antimicrob Agents Chemother* **59**: 1983-1991.

Lopez-Siles, M., Khan, T.M., Duncan, S.H., Harmsen, H.J., Garcia-Gil, L.J., and Flint, H.J. (2012) Cultured representatives of two major phylogroups of human colonic *Faecalibacterium prausnitzii* can utilize pectin, uronic acids, and host-derived substrates for growth. *Appl Environ Microbiol* **78**: 420-428.

Ludwig, W., Schleifer, K.-H., and Whitman, W.B. (2009) Revised road map to the phylum Firmicutes. In *Bergey's Manual® of Systematic Bacteriology: Volume Three The Firmicutes*. Vos, P., Garrity, G.M., Jones, D., Krieg, N.R., Ludwig, W., Rainey, F.A. et al. (eds). New York, NY: Springer New York, pp. 1-13.

Lytle, B., Myers, C., Kruus, K., and Wu, J.H.D. (1996) Interactions of the CelS binding ligand with various receptor domains of the *Clostridium thermocellum* cellulosomal scaffolding protein, CipA. *J Bacteriol* **178**: 1200-1203.

Miyazaki, K., Martin, J.C., Marinsek-Logar, R., and Flint, H.J. (1997) Degradation and utilization of xylans by the rumen anaerobe *Prevotella bryantii* (formerly *P. ruminicola subsp. brevis*) B(1)4. *Anaerobe* **3**: 373-381.

Monterroso, B., Saiz, J.L., Garcia, P., Garcia, J.L., and Menendez, M. (2008) Insights into the structure-function relationships of pneumococcal cell wall lysozymes, LytC and Cpl-1. *The Journal of biological chemistry* **283**: 28618-28628.

Morais, S., David, Y.B., Bensoussan, L., Duncan, S.H., Koropatkin, N.M., Martens, E.C. et al. (2016) Enzymatic profiling of cellulosomal enzymes from the human gut bacterium, *Ruminococcus champanellensis*, reveals a fine-tuned system for cohesin-dockerin recognition. *Environ Microbiol*. **18**: 542-556

Pastagia, M., Schuch, R., Fischetti, V.A., and Huang, D.B. (2013) Lysins: the arrival of pathogen-directed anti-infectives. *J Med Microbiol* **62**: 1506-1516.

Rincon, M.T., Martin, J.C., Aurilia, V., McCrae, S.I., Rucklidge, G.J., Reid, M.D. et al. (2004) ScaC, an adaptor protein carrying a novel cohesin that expands the dockerin-binding repertoire of the *Ruminococcus flavefaciens* 17 cellulosome. *J Bacteriol* **186**: 2576-2585.

Rogers, T.E., Pudlo, N.A., Koropatkin, N.M., Bell, J.S., Moya Balasch, M., Jasker, K., and Martens, E.C. (2013) Dynamic responses of *Bacteroides thetaiotaomicron* during growth on glycan mixtures. *Mol Microbiol* **88**: 876-890.

Schleifer, K.H., and Kandler, O. (1972) Peptidoglycan types of bacterial cell walls and their taxonomic implications. *Bacteriological reviews* **36**: 407-477.

Shah, H.N. (2013) The genus *Bacteroides* and related taxa. In *The Prokaryotes: A Handbook on the Biology of Bacteria*. Dworkin, M., Falkow, S., Rosenberg, E., Schleifer, K.-H., and Stackebrandt, E. (eds): Springer Science & Business Media.

Shugar, D. (1952) The measurement of lysozyme activity and the ultra-violet inactivation of lysozyme. *Biochim Biophys Acta* **8**: 302-309.

Sledjeski, D.D., and Gottesman, S. (1996) Osmotic shock induction of capsule synthesis in *Escherichia coli* K-12. *Journal of bacteriology* **178**: 1204-1206.

Sorg, J.A., and Dineen, S.S. (2009) Laboratory maintenance of *Clostridium difficile*. *Curr Protoc Microbiol* **Chapter 9**: Unit9A 1.

Torres-Cabassa, A.S., and Gottesman, S. (1987) Capsule synthesis in *Escherichia coli* K-12 is regulated by proteolysis. *Journal of bacteriology* **169**: 981-989.

Updyke, E.L., and Nickle, M.I. (1954) A dehydrated medium for the preparation of type specific extracts of group A *Streptococci*. *Appl Microbiol* **2**: 117-118.

Vollmer, W., Joris, B., Charlier, P., and Foster, S. (2008) Bacterial peptidoglycan (murein) hydrolases. *FEMS microbiology reviews* **32**: 259-286.

Wang, G., Olczak, A., Forsberg, L.S., and Maier, R.J. (2009) Oxidative stress-induced peptidoglycan deacetylase in *Helicobacter pylori*. *The Journal of biological chemistry* **284**: 6790-6800.

Wegmann, U., Louis, P., Goesmann, A., Henrissat, B., Duncan, S.H., and Flint, H.J. (2014) Complete genome of a new Firmicutes species belonging to the dominant human colonic microbiota ('*Ruminococcus bicirculans*') reveals two chromosomes and a selective capacity to utilize plant glucans. *Environ Microbiol* **16**: 2879-2890.

Whitfield, C., and Roberts, I.S. (1999) Structure, assembly and regulation of expression of capsules in *Escherichia coli*. *Mol Microbiol* **31**: 1307-1319.

Yaron, S., Morag, E., Bayer, E.A., Lamed, R., and Shoham, Y. (1995) Expression, purification and subunit-binding properties of cohesins 2 and 3 of the *Clostridium thermocellum* cellulosome. *FEBS Lett* **360**: 121-124.

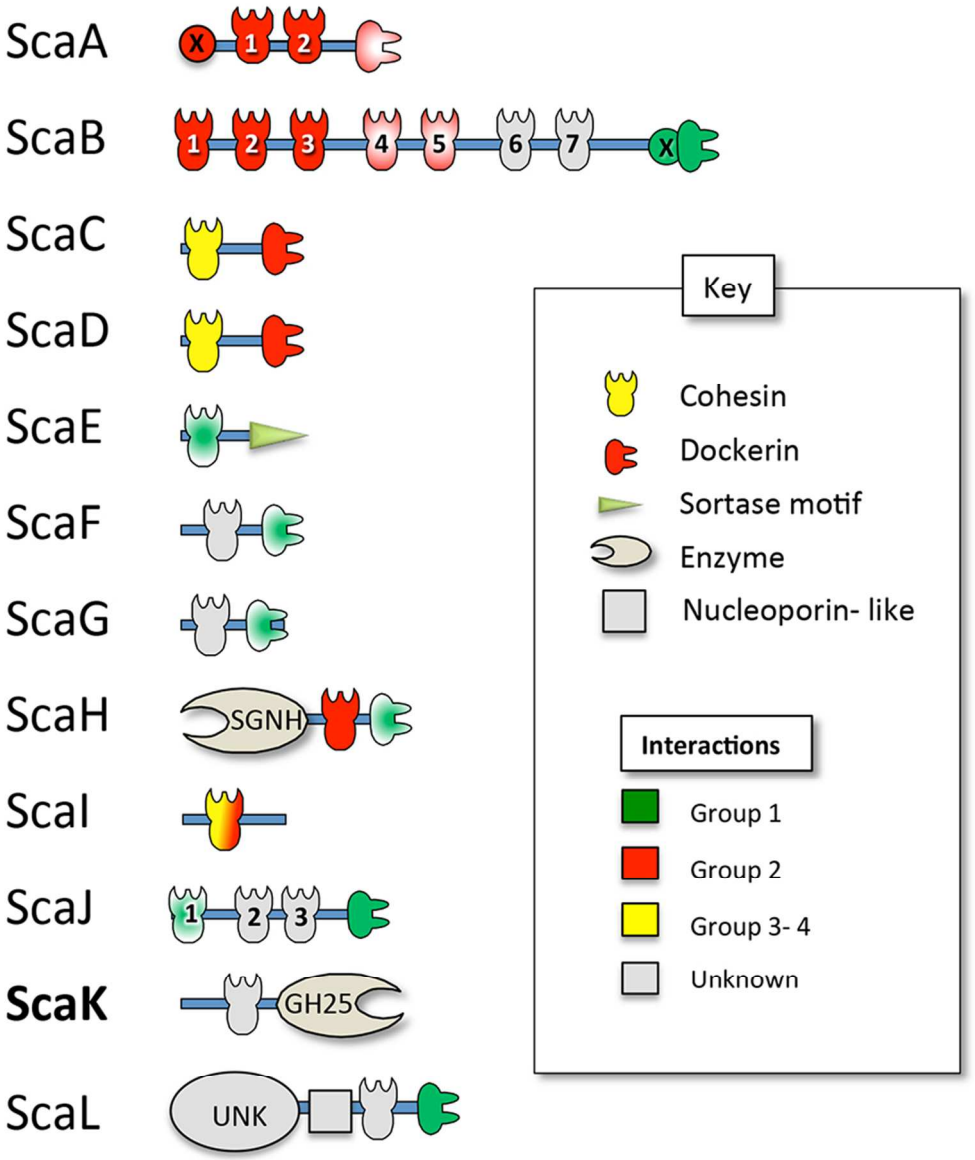

Figure 1: Schematic representation of the cohesin-bearing scaffoldin proteins in R. champanellensis based on the respective genome sequences. SGNH, hydrolase-type esterase domain (IPR013830); GH25, a putative GH25-family module sharing similarity to lysozyme. Specific interactions according to sequence alignment and biochemically characterized cohesin/dockerin interactions are color-coded. Shaded colors indicate that the designated cohesins or dockerins exhibit more selective interactions with only some of their Group 1 or Group 2 counterparts.
80x94mm (300 x 300 DPI)

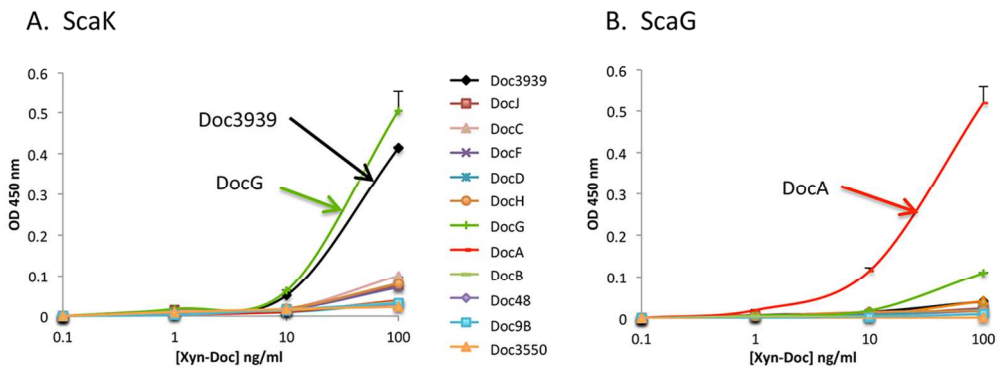

Figure 2: Newly discovered dockerin-binding profiles of R. champanellensis ScaK and ScaG cohesins measured by affinity ELISA (A) ELISA experiments demonstrating different interaction specificities between the ScaK cohesin and selected scaffoldin- and enzyme-borne dockerins. ScaK interacted with DocG and Doc3939 (B) ELISA experiments demonstrating different interaction specificities between the ScaG cohesin and selected scaffoldin- and enzyme-borne dockerins. ScaG interacted exclusively with DocA. Error bars indicate the standard deviation from the mean of triplicate samples (ELISA). The experiments were performed three times.
109x40mm (300 x 300 DPI)

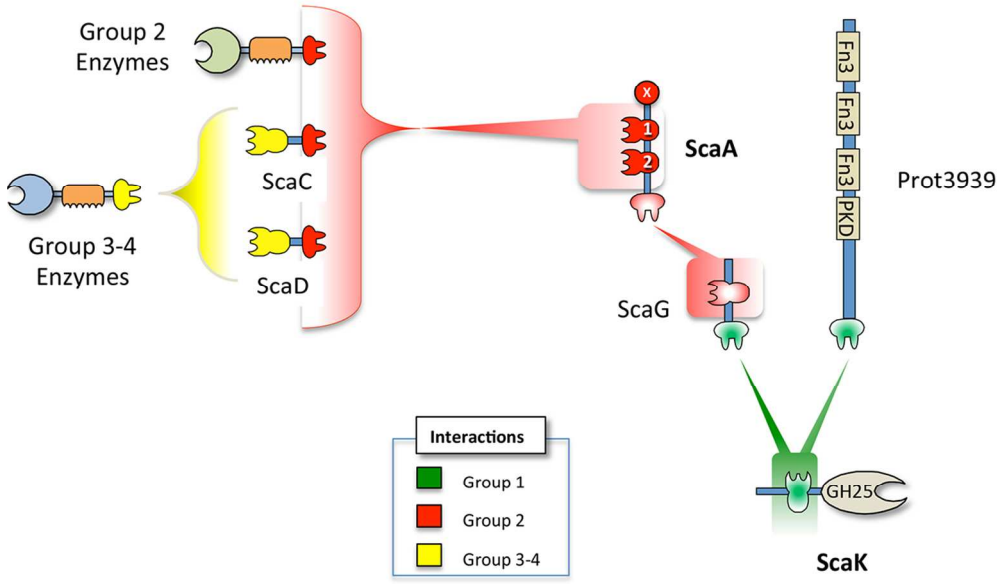

Figure 3: Proposed cell-free cellulosome complexes involving ScaK in R. champanellensis. Different types of cohesin-dockerin interactions are color-coded. The ScaK cohesin binds selectively to the dockerins of ScaG and Prot3939 and not to other Group 1 dockerins. Similarly, the ScaG cohesin appears to be very selective in its binding to the ScaA dockerin, and fails to bind other Group 2 dockerins.

109x65mm (300 x 300 DPI)

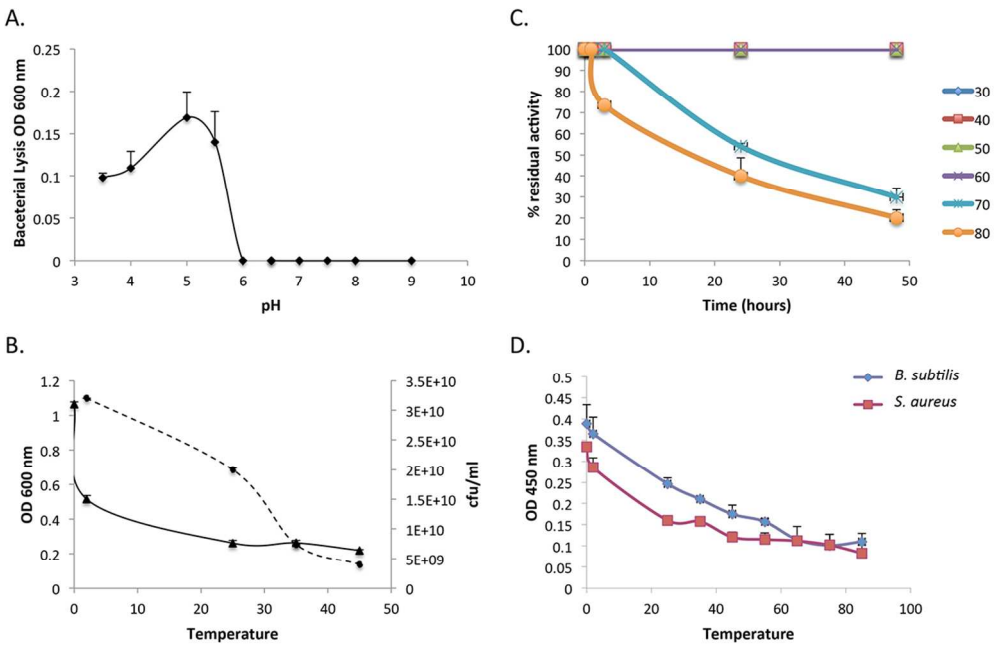

Figure 4: Characterization of recombinant R. champanellensis ScaK. (A) Effect of pH on lysozyme activity after 15 min incubation. (B) Thermostability of ScaK-derived lysozyme activity at different temperatures, following the heat-shock, the enzymatic activity was measured at pH 5 after 30 min incubation at 37°C. (C) Effect of temperature on lysozyme activity on E. coli cells at pH 5 after 30 min incubation, solid line representing the decrease in OD at 600 nm and dashed line, the viability of the cells (in cfu/ml) with the control counting 1.6.1012 cfu/ml. (D) Effect of temperature on lysozyme activity on the peptidoglycans of B. subtilis (blue line) and S. aureus (red line) at pH 5 after 30 min incubation. Enzymatic reactions, performed using the modified turbidimetric method were repeated in triplicate, and standard deviations are indicated.
109x71mm (300 x 300 DPI)